

A PRELIMINARY STUDY ON THE EXTRUSION RESOLUTION OF PLURONIC F127 FOR BIOPRINTING THERMO-RESPONSIVE HYDROGEL CONSTRUCTS

RATIMA SUNTORNNOND, JIA AN AND CHEE KAI CHUA
*Singapore Centre for 3D Printing, School of Mechanical and Aerospace Engineering,
Nanyang Technological University, 50 Nanyang Avenue, 639798, Singapore*

ABSTRACT: Thermo-responsive hydrogels have gained more attention recently due to their unique characteristic of tunable sol-gel transition when temperature is changed. They have been used for many biomedical applications from drug delivery to fabrication of soft tissue scaffolds via 3D bioprinting. In this paper, the preliminary investigation on bioprinted thermo-responsive hydrogels were conducted in order to find out the correlations between size of nozzle, stage moving speed and gas pressure for achieving optimum printing resolution. The hydrogel that was used in this study was pluronic F127 at 24.5 wt % concentration. Two sizes of nozzle were used (25G and 30G) while stage moving speed (printing speed) and gas pressure were designed to be three levels each. A total of 18 experiments were conducted. The results show that the thinnest continuous line (highest resolution) of hydrogel could be obtained even when a larger nozzle is used. This paper suggests a relationship of the main parameters with the size of nozzle on extrusion based bioprinter, and the results from this study may provide a platform for future correlation studies on extrusion based bioprinting.

KEYWORDS: Bioprinting; 3D printing; Thermo-responsive hydrogel printability; Pluronic F-127

INTRODUCTION

Bioprinting technology is an emerging technology that integrates additive manufacturing (also known as 3D printing) with biomaterials and living organisms to create suitable environment for cells to promote tissue growth *in vitro*. Bioprinting has been used for many applications from drug testing, cancer study, stem cell study to tissue engineering (TE). Bioprinting has brought many advantages to tissue engineering (TE). There are three main components of bioprinting which include (i) living cells, (ii) bioink or hydrogel and (iii) bioprinter machine (Knowlton, Onal, Yu, Zhao, & Tasoglu, 2015; Nakamura et al., 2015; Wang, Lee, & Yeong, 2015). For bioprinter, there are mainly three different types which are laser assisted based bioprinter, ink-jet based bioprinter and extrusion based bioprinter (An, Teoh, Suntoronnond, & Chua, 2015; Chua & Yeong, 2014; Lee & Yeong, 2015; Pereira & Bártolo, 2015). Among these three types, extrusion based bioprinter has the greatest capability to deal with the widest range of materials, due to the fact that it is able to dispense materials that have viscosity from 30 to 6×10^8 centipoise (mPa.s) (Jungst, Smolan, Schacht, Scheibel, & Groll, 2015; Knowlton et al., 2015). There are many hydrogels that have been used in biofabrication and bioprinting, including both natural and synthetic hydrogels, such as gelatin, alginate, polyethylene glycol (PEG) and pluronic (Malda et al., 2013; Suntoronnond, An, Yeong, & Chua, 2015; Tan & Yeong, 2015; Wang et al., 2015). Most of natural hydrogels have poor printability which makes it very hard to create 3D complex structure by directly bioprinting them. On the other hand, synthetic hydrogels has shown good printability e.g. pluronic F127. It has been proven that pluronic material has good printability and can be printed at low viscosity to high

viscosity. Thus, it is considered as one of the most versatile hydrogels that are easy to be printed and have good shape stability after printing (Chang, Boland, Williams, & Hoying, 2011; Müller, Becher, Schnabelrauch, & Zenobi-Wong, 2013). Although synthetic polymers can be biocompatible, they are usually not bioactive, meaning that they will not support cell growth for long term implantation (Suntornnond et al., 2015). Recently, Kolesky *et al.* showed that by using pluronic as a guided track for gelatin methacrylate (GelMA), a complex channel with cell encapsulation can be formed, which has a potential to be used for vascularized tissue engineering (Kolesky et al., 2014). However, the extrusion resolution of thermos-responsive hydrogels remains elusive and need more investigation. Thermos-responsive hydrogels are not only has high printability but also have good cell support environment. Therefore, in this paper, we further explored the relationship on extrusion based bioprinting parameters by using thermo-responsive hydrogel pluronic F127. In particular, the size of nozzle, feeding rate and gas pressure of a typical extrusion based bioprinter are focused.

MATERIALS AND METHODS

Pluronic F127 hydrogel preparation

Pluronic F127 (P2443) was purchased from Sigma-Aldrich, USA. Pluronic F127 is in white powder form. In order to make 24.5 wt % pluronic hydrogel, 12.25 grams of pluronic were mixed with 50 ml of deionized water under vigorous stirring at room temperature. After the solution was mixed and became homogeneous, 5 ml of Pluronic hydrogel were poured into the syringe before the actual printing.

Pluronic F127 hydrogel printing

Two different sizes of nozzle were used, 25G (inner diameter: 260 μm) and 30G (inner diameter: 159 μm). Three different levels of pressure (1, 2 and 3 bar) and three levels of stage moving speed (500, 1500 and 2500 mm/min) were studied in this printing experiment by using pneumatic extrusion based bioprinter (Regenhu, Switzerland). A total of 18 (2 x 3 x 3) experiments were investigated. Hydrogel was printed onto a clear glass slide, which is the platform for holding the printed structure.

Pluronic F127 hydrogel characterization

The widths of the printed lines in all 18 experiments were measured by using an optical microscope (Zeiss, Axio Vert.A1) with AxioCam (Cm1) at 5x magnification. In each experiment, three lines were printed as shown in Biocad drawing in Figure 1. In total, 54 data points were collected in this experiment.

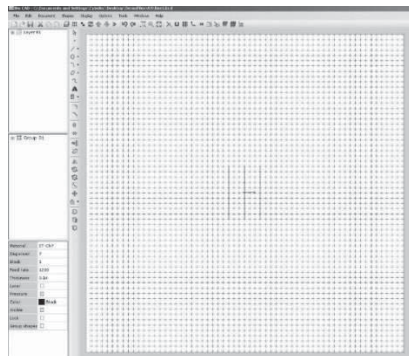


Figure 1. Biocad design for Pluronic F127 printing

RESULTS AND DISCUSSIONS

By using pluronic F127 at 24.5 %wt (viscosity approximately 30 mPa.s (Chang et al., 2011), the results (as summarized in Table 1 below) show that for 25G nozzle, the thinnest line was obtained at 1 bar and 2500 mm/min. For 30G nozzle, the thinnest line was obtained at 2 bar and 2500 mm/min. However, as shown in Figure 2c, at 2500 mm/min, the lines were not continuous after printing. In general, at a higher printing speed, discontinuities and variation in line width would occur, while at a lower feed rate, the lines became wider as shown in Figure 2a. Therefore, in order to obtain the thinnest continuous line, the printing speed of 1500 mm/min is preferable for both nozzle sizes (as shown in Figure 2b).

Table 1. Line width results from extrusion based bioprinter in micrometre (μm)

| | Stage moving speed (mm/min) | Pressure (bar) | | |
|------------------------------------|-----------------------------|----------------|-----------------|-----------------|
| | | 1 | 2 | 3 |
| 25G (260 μm) | 500 | 503.7 \pm 22 | 2457.1 \pm 15 | 4042.6 \pm 71 |
| | 1500 | 318.5 \pm 12 | 761.5 \pm 4 | 1324.4 \pm 79 |
| | 2500 | 294.2 \pm 14 | 562.1 \pm 19 | 889.6 \pm 38 |
| | | | | |
| 30G (159 μm) | | Pressure (bar) | | |
| | | 1 | 2 | 3 |
| | 500 | N/A | 380.3 \pm 5 | 1043.2 \pm 16 |
| | 1500 | N/A | 192.5 \pm 7 | 507.9 \pm 15 |
| | 2500 | N/A | 146.4 \pm 27 | 297.6 \pm 59 |

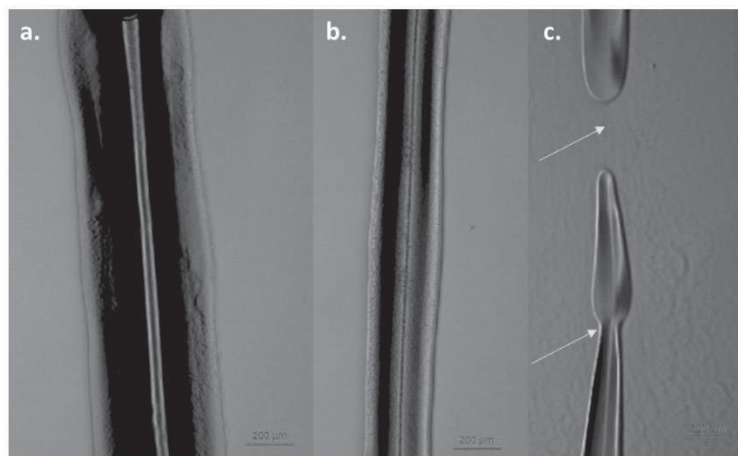


Figure 2. Line width by using 25G nozzle at 1 bar and different feed rate: a) 500 mm/min, b) 1,500 mm/min and c) 2,500 mm/min (the arrows indicate defects of the printed line and scale bar is 200 μm)

As shown in Figure 3, the effect of pressure shows that at a higher pressure, the line width become wider especially when the stage moving speed is low. In this case, in order to obtain a fine printing line, the pressure needs to be low enough to extrude a minimal amount of material out of the nozzle. As expected, for a smaller nozzle, a higher pressure is required to overcome the effect of capillary force. At the highest stage moving speed, the thinnest line can be fabricated. These results are in agreement with the results from Müller *et al.*, in which a micro-valve based nozzle was used to print sacrificial pluronic mould (Müller *et al.*, 2013).

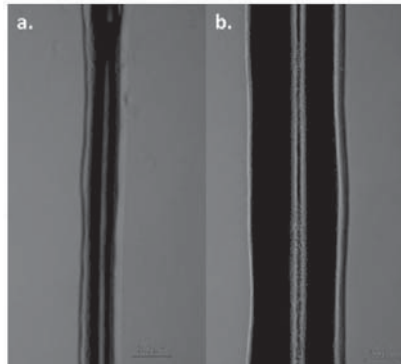


Figure 3. Line width by using 30G nozzle at 1500 mm/min and different pressures: a) 2 bar and b) 3 bar (scale bar is 200 μm)

Another interesting observation is that at a higher stage moving speed the smaller nozzle printed a more defected line than the larger nozzle, as shown in Figure 4 below. This is due to a less amount of materials extruded from the smaller nozzle. For 30G at 2500 mm/min and 3 bar, not only the printed line was discontinuous, but also the change in the shape of the printed line was drastic (Figure 4a).

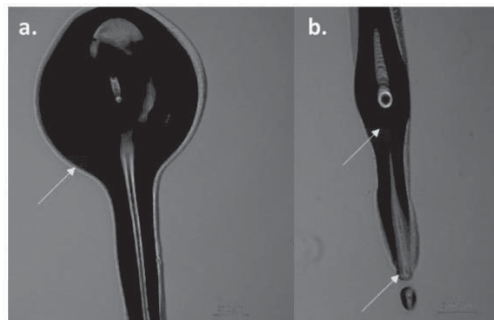


Figure 4. Defect from the printed lines using 30G nozzle at 3 bar 2500 mm/min: a) The defect at the starting point of the line and b) The defect at the ending point of the line (the arrows pointed the defects and scale bar is 200 μm)

For 25G nozzle, the optimum printing conditions should be 1500 – 2500 mm/min and at 1-2 bar. For 30G nozzle, the optimum printing conditions should be 500 – 1,500 mm/min and at 2-3 bar. Therefore, in order to obtain the finest (or smallest) continuous line, a lower pressure and a faster stage moving speed are required for a bigger nozzle size. Based on these preliminary results,

empirical equations are obtained to estimate the pressure and stage moving speed for other sizes of nozzle as demonstrated below

$$\text{Pressure: } f_p(x) = \begin{cases} f_{p,\min} = 3.5743 - 0.001x \\ f_{p,\max} = 4.5743 - 0.001x \end{cases} \quad \text{when } 0 < x < 3574 \quad (1)$$

$$\text{Stage moving speed: } f_v(x) = \begin{cases} f_{v,\min} = -(1,074.257 - 9.901x) \\ f_{v,\max} = -(74.257 - 9.901x) \end{cases} \quad \text{when } 108.5 < x < 1017.5 \quad (2)$$

where x is a size of nozzle in micrometre (μm)

The equations are derived from curve fitting using OriginPro (version 8.5) as shown in Figure 5 below, without considering the effect of the combination of pressure and printing speed. The condition is to confirm that the pressure will not reach 0 value and stage moving speed will not exceed maximum limit. The 3D data are simplified to two 2D curve so that the equations can be derived. This study has provided a platform for future correlation studies on extrusion based bioprinting of thermos-responsive hydrogel. However, the equations above are only applicable to material that has viscosity around 30 mPa·s and still need further validation on other different sizes of nozzle. In the future, more focus will be on equation validation and modification, so as to further expand this equation with the relationship of material viscosity with nozzle size, pressure and stage moving speed. Moreover, more data need to be obtained to create a surface plot for more precise equations to estimate initial pressure and stage moving speed. This extrusion based printing study is not only important for bioprinting but may also be applied to other 3D printing technologies such as fused deposition modelling (FDM), chocolate printing or even 4D printing technology (An, Chua, & Mironov, 2016; Khoo et al., 2015).

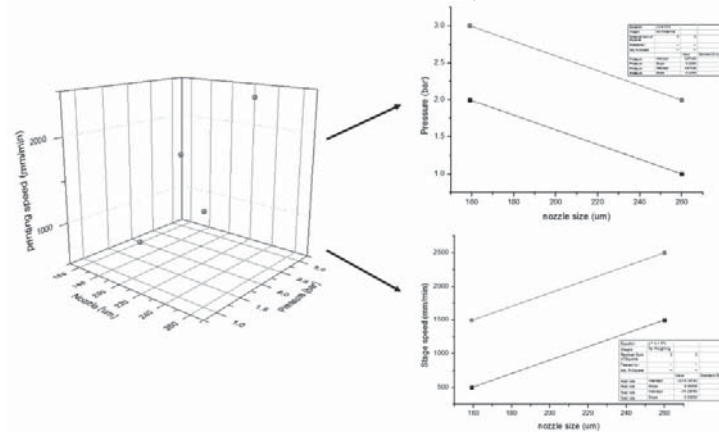


Figure 5. 3D graph was simplified to 2D graph for curve fitting from at optimum printing conditions of 25G and 30G nozzles

CONCLUSIONS

The relationship between size of nozzle with pressure and stage moving speed was studied by using pluronic F-127 at 24.5 %wt. The results show that even though the fastest stage moving speed and lowest pressure provided the thinnest line, the lines from this condition have many defects which include gaps along the line and line shape inconsistency. Moreover, it is found that

for a smaller nozzle, a higher pressure is needed but stage moving speed should be reduced to prevent printing defected lines. Empirical equations are suggested to provide a preliminary basis for selecting from a range of pressures and stage moving speeds for printing hydrogel of 30 mPa.s viscosity for different size of nozzle. Therefore the results from this study may provide a preliminary platform for extrusion based printing to create guided track or mould, which could lead to further advancement in 3D bioprinting and cell patterning study.

ACKNOWLEDGMENTS

Singapore Centre for 3D Printing is supported by Singapore National Research Foundation (NRF).

REFERENCES

- An, J., Chua, C. K., & Mironov, V. (2016). A perspective on 4D bioprinting. *International Journal of Bioprinting*, 2.
- An, J., Teoh, J. E. M., Suntornnond, R., & Chua, C. K. (2015). Design and 3D Printing of Scaffolds and Tissues. *Engineering*, 0.
- Chang, C. C., Boland, E. D., Williams, S. K., & Hoying, J. B. (2011). Direct-write bioprinting three-dimensional biohybrid systems for future regenerative therapies. *Journal of Biomedical Materials Research Part B: Applied Biomaterials*, 98(1), 160-170.
- Chua, C. K., & Yeong, W. Y. (2014). *Bioprinting: principles and applications*: World Scientific.
- Jungst, T., Smolan, W., Schacht, K., Scheibel, T., & Groll, J. r. (2015). Strategies and Molecular Design Criteria for 3D Printable Hydrogels. *Chemical Reviews*.
- Khoo, Z. X., Teoh, J. E. M., Liu, Y., Chua, C. K., Yang, S., An, J., . . . Yeong, W. Y. (2015). 3D printing of smart materials: A review on recent progresses in 4D printing. *Virtual and Physical Prototyping*, 10(3), 103-122. doi: 10.1080/17452759.2015.1097054
- Knowlton, S., Onal, S., Yu, C. H., Zhao, J. J., & Tasoglu, S. (2015). Bioprinting for cancer research. *Trends in Biotechnology*, 33(9), 504-513. doi: <http://dx.doi.org/10.1016/j.tibtech.2015.06.007>
- Kolesky, D. B., Truby, R. L., Gladman, A., Busbee, T. A., Homan, K. A., & Lewis, J. A. (2014). 3D bioprinting of vascularized, heterogeneous cell-laden tissue constructs. *Advanced Materials*, 26(19), 3124-3130.
- Lee, J. M., & Yeong, W. Y. (2015). A preliminary model of time-pressure dispensing system for bioprinting based on printing and material parameters: This paper reports a method to predict and control the width of hydrogel filament for bioprinting applications. *Virtual and Physical Prototyping*, 10(1), 3-8.
- Malda, J., Visser, J., Melchels, F. P., Jüngst, T., Hennink, W. E., Dhert, W. J., . . . Huttmacher, D. W. (2013). 25th anniversary article: engineering hydrogels for biofabrication. *Advanced Materials*, 25(36), 5011-5028.
- Müller, M., Becher, J., Schnabelrauch, M., & Zenobi-Wong, M. (2013). Printing thermoresponsive reverse molds for the creation of patterned two-component hydrogels for 3D cell culture. *Journal of visualized experiments: JoVE*(77).
- Nakamura, M., Mir, T. A., Arai, K., Ito, S., Yoshida, T., Iwanaga, S., . . . Nikaido, T. (2015). Bioprinting with pre-cultured cellular constructs towards tissue engineering of hierarchical tissues. *International Journal of Bioprinting*, 1, 39-48. doi: <http://dx.doi.org/10.18063/IJB.2015.01.007>
- Pereira, R. F., & Bártolo, P. J. (2015). 3D bioprinting of photocrosslinkable hydrogel constructs. *Journal of Applied Polymer Science*, 132(48).
- Suntornnond, R., An, J., Yeong, W. Y., & Chua, C. K. (2015). Biodegradable Polymeric Films and Membranes Processing and Forming for Tissue Engineering. *Macromolecular Materials and Engineering*, 300(9), 858-877. doi: 10.1002/mame.201500028
- Tan, E. Y. S., & Yeong, W. Y. (2015). Concentric bioprinting of alginate-based tubular constructs using multi-nozzle extrusion-based technique. *International Journal of Bioprinting*, 1(1), 49-56.
- Wang, S., Lee, J. M., & Yeong, W. Y. (2015). Smart hydrogels for 3D bioprinting. *International Journal of Bioprinting*, 1(1).